

# INTERNATIONAL SOCIETY FOR SOIL MECHANICS AND GEOTECHNICAL ENGINEERING



*This paper was downloaded from the Online Library of the International Society for Soil Mechanics and Geotechnical Engineering (ISSMGE). The library is available here:*

<https://www.issmge.org/publications/online-library>

*This is an open-access database that archives thousands of papers published under the Auspices of the ISSMGE and maintained by the Innovation and Development Committee of ISSMGE.*

*The paper was published in the proceedings of the 20<sup>th</sup> International Conference on Soil Mechanics and Geotechnical Engineering and was edited by Mizanur Rahman and Mark Jaksa. The conference was held from May 1<sup>st</sup> to May 5<sup>th</sup> 2022 in Sydney, Australia.*

## Evaluation of the Material Point Method for the modeling of suffusion processes

### Évaluation de la méthode du point matériel pour la modélisation des processus de suffusion

**Alba Yerro**

*Department of Civil and Environmental Engineering, Virginia Tech, USA, [ayerro@vt.edu](mailto:ayerro@vt.edu)*

**John Murphy**

*US Army Engineering Research and Development Center, Vicksburg, USA, [john.w.murphy@usace.army.mil](mailto:john.w.murphy@usace.army.mil)*

**Kenichi Soga**

*Department of Civil and Environmental Engineering, University of California, Berkeley, USA*

**ABSTRACT:** Internal erosion of soils, or the mobilization of solid particles as water flows through the granular material, is a critical geotechnical hazard that affects the stability of earth dams and levees. These soils usually have a bimodal nature, in which a finer fraction is eroded and transported through the voids in the matrix of coarser particles. When the erosion is non-destructive, and the internal structure of the soil remains intact, the process is so-called suffusion. The Material Point Method (MPM) has shown promise in modeling large deformation in multi-phase geotechnical problems. Recently, two different MPM formulations have been proposed to study the internal erosion of bimodal soils. One with a single set of material points (MPs) represents solid and liquid phases, and the second one with two sets of MPs, one set for each phase. In both formulations, the internal erosion mechanism is represented by transferring mass between the solid and liquid phases, and an erosion law controls the rate of mass transfer. This work compares the two approaches and discusses their applicability in geotechnical problems that involve seepage and internal erosion. In particular, both approaches are verified with the analytical results of a theoretical constant-head suffusion test. The performance of the numerical model is evaluated for different discretizations. Mass conservation is fulfilled for both formulations.

**RÉSUMÉ:** L'érosion interne des sols, ou la mobilisation de particules solides lorsque l'eau s'écoule à travers le matériau granulaire, est un danger géotechnique critique qui affecte la stabilité des barrages en terre et des digues. Ces sols ont généralement une nature bimodale, dans laquelle une fraction plus fine est érodée et transportée à travers les vides de la matrice de particules plus grossières. Lorsque l'érosion est non destructive et que la structure interne du sol reste intacte, le processus est ce qu'on appelle la suffusion. La méthode du point matériel (MPM) s'est révélée prometteuse dans la modélisation de grandes déformations dans des problèmes géotechniques à phases multiples. Récemment, deux formulations MPM différentes ont été proposées pour étudier l'érosion interne des sols bimodaux. L'un avec un seul ensemble de points matériels (MP) représente les phases solides et liquides, et le second avec deux ensembles de MP, un ensemble pour chaque phase. Dans les deux formulations, le mécanisme d'érosion interne est représenté par le transfert de masse entre les phases solide et liquide, et une loi d'érosion contrôle la vitesse de transfert de masse. Cet article compare les deux approches et analyse/présente/adresse leur applicabilité à des problèmes géotechniques impliquant des infiltrations et une érosion interne. En particulier, les deux approches sont validées avec les résultats analytiques d'un test théorique de suffusion à tête constante. Les performances du modèle numérique sont évaluées pour différentes discrétisations. La conservation de masse est satisfaite pour les deux approches.

**KEYWORDS:** Internal erosion, suffusion, material point method, large deformations.

## 1 INTRODUCTION

Internal erosion can cause the failure of water retention structures which can result in catastrophic damage in the downstream areas. The development of numerical approaches capable of capturing internal erosion and post-failure consequences is extremely challenging because it requires advanced formulations capable of dealing with hydro-mechanical coupling, soil-structure interaction, and large deformations of the material involved.

In the geotechnical field, "internal erosion" is used as a generic term to describe the erosion of soil particles by water passing through a porous soil matrix. The process can be generally broken into four stages: (1) initiation or particle detachment, (2) continuation or inadequate particle retention, (3) progression including particle transport and enlargement of the erosion pathway, and (4) initiation of a possible breach. In this paper, we strictly focus on the three first stages.

Different modes of internal erosion can be distinguished among others: "internal instability," "piping," or "sand production." Internal instability is a non-localized phenomenon whereby fine particles are transported through the voids of the solid matrix during seepage flow (Fannin & Slangen 2014). When this leads to the deformation of the solid skeleton or even

to a final collapse of the washed-out soil structure, the term "suffusion" is used. On the contrary, the term "suffusion" is used by many authors to describe the particular case when the internal instability process is non-destructive, and the internal structure of the soil remains intact. Numerous experimental techniques have been developed in order to reproduce internal erosion phenomena in internally unstable soils (e.g., Skempton & Brogan 1994; Sterpi 2003; Indraratna et al. 2011; Zhong et al 2018). Many of them consist of rigid-wall permeameter tests in which a one-dimensional water flow is imposed through the sample, and the eroded particles escaping the soil are collected from the outflow.

The term "piping" involves the progressive erosion and transportation of soil grains along a localized flow path, forming a continuous channel of high permeability that, in some cases, can connect upstream and downstream sides of the water retaining structure, leading to a general failure. In the field of geomechanics, several laboratory methods have been developed for simulating the piping erosion process experimentally, with particular attention focused on the hole erosion test (e.g., Wan & Wang 2002). A review on soil piping was presented by Richards & Reddy (2007), and several laboratory works are available in

the literature (e.g., van Beek et al 2014). According to these previous definitions, it is important to note that different erosion modes can be closely related. Suffosion occurring within a foundation of a dam can be the triggering factor of piping, which in turn may result in a catastrophic failure of the structure. The study of internal erosion also appears in oil-producing wells and is a current research field in hydrocarbon and petroleum engineering (e.g., Vardoulakis et al. 1996, Subbiah et al. 2020). "Sand production" is the concept used in this field to describe the migration of the formation of sand induced by the flow of reservoir fluids.

Within the last 25 years, numerical methods in the framework of continuum mechanics, such as the Finite Element Method (FEM) and the Finite Difference Method (FDM), have been used to analyze internal erosion problems. Vardoulakis et al (1996) set the first model to study the hydro-mechanical aspect of the sand production problem. This approach concentrates on the simulation of the mass transport phenomenon by means of a three-phase mixture theory consisting of solid skeleton, fluidized solids (i.e., eroded grains), and fluid. The deformation of the solid skeleton is neglected, and the constitutive coupling between erosion and soil weakening is ignored. Stavropoulou et al (1998) extended the work from Vardoulakis et al (1996) and presented the first attempt to couple erosion to mechanical damage of soil or rock around a wellbore. After those developments, a number of numerical formulations in different numerical frameworks have been proposed (e.g., Benseghier et al 2020). In particular, the Material Point Method (MPM) has been recently extended to simulate internal erosion in bi-modal saturated soils (Yerro et al 2017; Murphy et al 2020). One of the strengths of the MPM is the capability of simulating large deformations of history dependent materials without mesh tangling typical from mesh-based methods (e.g., FEM, FDM). This characteristic can be extremely useful to study in a unique calculation the stability and runoff consequences of internal erosion triggered failures of water retaining structures.

This work aims to compare the two MPM formulations recently proposed for the simulation of internal erosion processes and to discuss the effects of different initial material discretization on the final solution. All the simulations presented in this analysis are performed assuming rigid soil skeleton. Understanding the limitations of the different approaches using simplified soil behavior is essential before accounting for the coupling between internal erosion and soil deformation. Particular attention is provided to the definition of boundary conditions. To accomplish this objective, the paper is organized as follows. First, we define internal erosion processes in bimodal soils. Then, we introduce the basis of MPM and present the two MPM formulations. Finally, a numerical example consisting of a one-dimensional downward water flow is used to verify the implementation of both formulations. Results are presented and discussed using two erosion laws. Final conclusions are summarized in the end.

The models presented in this paper have been obtained with a version of the open-source Anura3D software (Anura3D, 2021).

## 2 INTERNAL EROSION IN BIMODAL SOILS

The solid phase of internally unstable soils is formed by a solid matrix, i.e., coarse grains and fine grains. While total stresses are mainly carried by the coarse grains, the fine grains remain under lower confinement, and, as a result, they are susceptible to erosion when the system is subjected to certain hydraulic conditions (Skempton and Brogan, 1994). The liquid phase contains water, and fluidized grains eroded from the fine fraction and can move with respect to the solid phase. Figure 1 presents the phase diagram for a reference volume of bimodal soil subjected to suffosion. The volumetric concentration ratios of the liquid phase ( $n_L$ ), solid phase ( $n_S$ ), solid skeleton ( $n_C$ ), erodible

grains ( $n_e$ ), fluidized grains ( $n_f$ ), and water ( $n_w$ ) are indicated. Note that  $n_L$  is a measure of porosity. Curved arrows indicate the direction of mass exchange of fine grains between solid and liquid phases.  $\vec{v}_L$  and  $\vec{v}_S$  represent the velocity of liquid and solid phases, respectively.

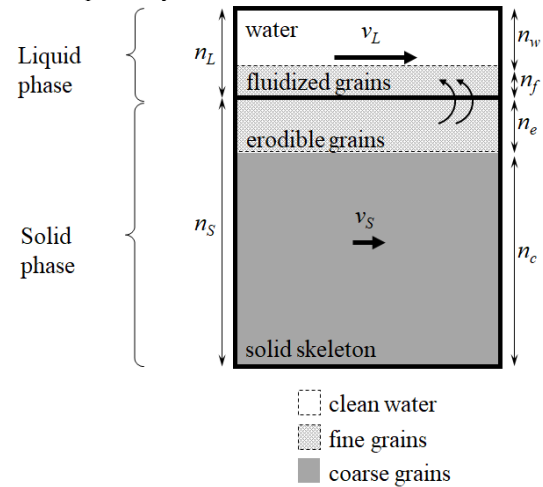


Figure 1. Phase diagram of the suffosion process in a reference volume of a bimodal soil specimen.

## 3 MPM FOR INTERNAL EROSION

The Material Point Method (MPM) is a particle-based numerical tool that is well suited to simulate large deformations. It was initially proposed by Sulsky et al (1994) in the field of solid mechanics, and in the last fifteen years, it has been further developed to address hydro-mechanical problems in the geotechnical field. MPM discretizes the material with a set of independent integration points, so-called material points (MPs) that carry the information (e.g., mass, strain, stress, velocity) and moves attached to the continuum. The main governing equations, traditionally the dynamic momentum balances, are solved at the nodes of a computational mesh that usually remains fixed during the calculation. Nodal unknowns (i.e., acceleration or linear momentum) are transferred back to the MPs, and the velocity and position are updated. Finally, compatibility equations, mass balances, and constitutive laws are posed at the MPs at the end of the computational cycle to update secondary variables. The whole computational cycle is commonly integrated explicitly in time, which means that the solution is conditionally stable. The advantages and limitations of this method for the simulation of large deformations in the geotechnical field are discussed in Soga et al (2015).

Two different hydro-mechanical MPM formulations are available for the study of fully saturated soils and seepage problems: the two-phase single-point formulation (SP) (e.g., Al-Kafagi 2013) and the two-phase double-point formulation (DP) (e.g., Bandara and Soga, 2015; Martinelli 2016). Both approaches consider coupled two-phase hydro-mechanical frameworks to represent the interactions between the solid skeleton and porous liquid. The most relevant difference is that SP uses one single set of MPs to represent the saturated media. In contrast, DP represents the solid and liquid phases separately with two completely different sets of MPs (i.e., so-called solid material points, SMPs, and liquid material points, LMPs). The SMPs represent the solid phase, and LMPs represent the liquid phase (either free fluid or porous fluid). When SMPs and LMPs are present in the same element, the element is considered to be in saturated conditions. Otherwise, the element is considered either dry soil or free liquid if only SMPs or LMPs are present, respectively. The mass conservation in DP is automatically fulfilled, while in the SP approach, the conservation of the liquid mass depends on the accuracy of the solution when solving the

liquid mass balance. While the DP is computationally less efficient than the SP due to more MPs required to run an equivalent model, the DP offers the advantage of being able to model free surface flow. A comparison between the two formulations is presented in detail by Ceccato et al (2018).

Standard SP and DP formulations neglect any mechanism involving the mass exchange between solid and liquid components. To overcome this limitation, both formulations have been recently extended to account for the mass transfer that takes place during internal erosion processes (Yerro et al 2017, Murphy et al 2020). In particular, mechanisms of particle detachment are controlled by the addition of an erosion law that governs the rate of eroded mass transferred from the solid skeleton to the liquid phase. Processes of particle retention (solid grains transported by the liquid that are retained by the solid skeleton) are not considered but could be included by adding a deposition law that controls the rate of mass moving from liquid to solid phases.

The hypothesis considered in both formulations include (a) fluidized grains move together with the water with a common velocity  $\vec{v}_L$ , (b) solid grains are incompressible, (c) erosion of coarse fraction is not permitted, (d) deposition processes are neglected, (e) liquid phase is weakly compressible, and (f) effect of temperature is neglected. In the following subsections, we summarize the extended SP and DP approaches, present the erosion laws considered in this work, and discuss the mass transfer process in both approaches.

### 3.1 Two-phase single-point (SP) approach for internal erosion

The first attempt to solve internal erosion problems in MPM was proposed by Yerro et al (2017). They extended the SP framework proposed by Al-Kafagi (2013). Very recently, the same approach has been extended for the simulation of internal erosion in partially saturated soils (Lei et al 2020). The main governing equations consist of the dynamic momentum balances of the liquid phase and the mixture. Laminar flow is considered and Darcy's law is assumed to evaluate drag forces (interaction force between solid and liquid) in the dynamic momentum balance of the liquid. The two momentum balances, discretized at the nodal mesh, remain essentially the same as in Al-Kafagi (2013). Contrarily, the mass balances are modified to account for the internal erosion processes as follows. In particular, the mass balance of the solid phase (Eq. 1), written in terms of porosity ( $n_L$ ) increase, includes an additional term to account for the volume erosion rate ( $\phi_e$ ). The mass balance of the water (Eq. 2) is now written in terms of the volumetric concentration ratio of the water ( $n_w$ ) and represents the volumetric deformation of the liquid phase ( $\epsilon_{volL}$ ). Note that the standard SP neglects the advective fluxes due to porosity gradients while this formulation preserves them to ensure mass conservation (third term of Eq. 2). Finally, the mass balance of the fluidized grains (Eq. 3) is added to evaluate the increment of volumetric concentration ratio of fluidized grains ( $n_f$ ), consistent with the volume erosion rate. The three mass balances are posed at the same set of MPs, which in this case, all represent a portion of the saturated media and contain information from both liquid and solid phases. Compatibility equations and constitutive equations are also posed at the MPs (Yerro et al 2017).

$$\frac{D^S n_L}{Dt} = n_S \nabla \cdot \vec{v}_S + \phi_e \quad (1)$$

$$\frac{D^S \epsilon_{volL}}{Dt} = \frac{1}{n_w} [n_S \nabla \cdot \vec{v}_S + n_L \nabla \cdot \vec{v}_L + (\vec{v}_L - \vec{v}_S) \cdot \nabla n_L] \quad (2)$$

$$\frac{D^S n_e}{Dt} = -n_e \nabla \cdot \vec{v}_L - (\vec{v}_L - \vec{v}_S) \cdot \nabla n_e + \phi_e \quad (3)$$

In the previous equations, all material derivatives are written with respect to the solid phase ( $\frac{D^S}{Dt}$ ) because all MPs describe the Lagrangian motion of the solid skeleton.

### 3.2 Two-phase double-point (DP) approach for internal erosion

The DP approach proposed by Martinelli (2016) has been recently extended by the authors of this paper to model internal erosion (Murphy et al 2020). In this framework, the liquid and solid dynamic momentum balances are posed at the nodal mesh using information from LMPs and SMPs. The drag forces in both momentum balances account for the high-velocity regime (Martinelli, 2016).

The mass balances are extended to account for the mass exchange resulting from internal erosion processes. The mass balance of the solid is identical to that of SP (Eq. 1). The mass balance of the liquid phase and the mass balance of fluidized grains are written as Eq. 4 and 5, respectively. Note that Eq. 4 and Eq. 5 differ from Eq. 2 and 3 because in the DP approach, the liquid motion is represented by a separate set of LMPs, and consistently, the liquid material derivative ( $\frac{D^L}{Dt}$ ) is accounted for.

$$\frac{D^L \epsilon_{volL}}{Dt} = \frac{1}{n_w} [(1 - n_w) \nabla \cdot \vec{v}_S + n_w \nabla \cdot \vec{v}_L + (\vec{v}_L - \vec{v}_S) \cdot \nabla n_L] \quad (4)$$

$$\frac{D^L n_e}{Dt} = -n_e \nabla \cdot \vec{v}_S + \phi_e \quad (5)$$

### 3.3 Evaluation of the erosion law and mass transfer in SP and DP approaches

The erosion law is required to evaluate the rate of eroded volume ( $\phi_e$ ) from the solid phase. In general, the erosion law describes the initiation of grain detachment based on macro-scale criteria, such as the amount of erodible grains remaining in the soil ( $n_e$ ), porosity, fluid velocity, concentration of fluidized grains, among others (Vardoulakis et al 1996; Cividini & Gioda 2004; Sterpi 2003). Because the primary purpose of this paper is not to exactly reproduce experimental data but to theoretically compare extended SP and DP formulations, two simplified erosion laws are considered. The first one (Eq. 6) represents a constant rate of eroded volume. The second one (Eq. 7) depends on the natural logarithm of the ratio between current and maximum porosity ( $n_L$  and  $n_{L,max}$ , respectively). The maximum porosity  $n_{L,max}$  is the porosity assuming that all erodible grains are washed out from the soil specimen. Note that this law implicitly depends on the amount of erodible grains remaining in the soil; the erosion rate decreases when internal erosion progresses, and less erodible mass remains in the soil specimen. This non-constant erosion law was selected for convenience to show a non-linear erosion process with time.

$$\phi_e = \alpha \quad (6)$$

$$\phi_e = -\beta \ln \frac{n_L}{n_{L,max}} \quad (7)$$

While the same erosion law can be considered in SP and DP frameworks, its evaluation and consequent mass transfer is different. Because MPs in the SP approach carry solid and fluid phases information, the rate of eroded volume ( $\phi_e$ ) and mass transfer are all evaluated at the same MPs in terms of volumetric concentration ratios. The eroded mass is transferred from the solid to the liquid phases and transported across with the liquid using an Eulerian description of the motion (the motion is described with respect to the solid skeleton in terms of in/outflow).

The DP approach evaluates  $\phi_e$  only at the SMPs. Then,  $\phi_e$  is transformed to eroded mass (multiplying by the density of the solid grains and the reference volume of the SMPs). Finally, the eroded masses from all SMPs in each element are summed together and equally distributed to the LMPs present in the same element. This information exchange between SMPs and LMPs is required to reproduce the mass transfer between solid and mass phases. Once the eroded mass is carried by the LMPs (i.e.,

fluidized grains), its motion is described using a Lagrangian description, and the trajectory of the fluidized grains is tracked.

#### 4 NUMERICAL MODEL

The models are inspired by constant head laboratory suffusion tests (e.g., Sterpi 2003). Still, the aim of the following sections is not to reproduce experimental results but to compare SP and DP performance and verify the results with analytical solutions. The model simulates one-dimensional downward vertical water flow through a squared bimodal soil specimen (1m x1m). Clean water enters the top of the model, passes through the soil block accumulating eroded mass, and exits the bottom of the soil boundary.

The gravity is not considered and the flow is prescribed by inducing a constant hydraulic gradient. As a result, the direction of the flow (either downward or upward) does not have an impact on the results. Because of the different nature of the SP and DP approaches, the boundary conditions are applied differently. The flow is assumed to be laminar. All models assume constant permeability for simplification purposes but could be easily updated during the calculation to account for porosity changes. The solid skeleton is assumed fixed, which is consistent with the suffusion process. This means that all MPs in the SP model and all SMPs in the DP model remain fixed during the calculation. The concentration ratio of the solid skeleton ( $n_c$ ) sets the minimum concentration ratio of the solid skeleton. When the concentration ratio of solid mass is exceeded, erosion is no longer allowed. Both models are explicitly integrated, and a time step of 0.0851 seconds is used to ensure the stability of the solution. A mass scaling factor of 10000 is used to optimize the calculation time (Al-Kafagi 2013). All computational meshes consist of linear triangular elements.

Table 1 shows the model material parameters used in this study. The erosion parameters concentration ratio of the soil skeleton,  $\alpha$ , and  $\beta$  are selected to speed up the calculation (erosion is complete around or before 100 seconds) while demonstrating the capability of the SP and DP formulations.

Table 1. General Model Material Parameters

Material Parameter [units]	Single-point (SP)	Double-point (DP)
Initial porosity [-]	0.3	0.3
Concentration ratio of the soil skeleton [-]	0.6	0.6
Density solid grains [kg/m <sup>3</sup> ]	2700	2700
Density water [kg/m <sup>3</sup> ]	1000	1000
Permeability [m/s]	2e-2	2e-2
Bulk modulus of water [kPa]	20000	20000
$\alpha$ (parameter Eq. 6) [s <sup>-1</sup> ]	1e-3	1e-3
$\beta$ (parameter Eq. 7) [s <sup>-1</sup> ]	1e-2	1e-2

##### 4.1 Single-point numerical model

This section covers the details specific to the SP model. The model is 2D and essentially consists of the soil specimen. The nominal mesh size is 0.25m, and the number of MPs per element is 3. The MPs are initialized at the Gauss points of each element. Their position is fixed throughout the simulation. The model is calculated using Mixed Integration (Al-Kafagi 2013).

The flow through the soil block is driven by applying a pore-pressure boundary condition at the top of the soil block ( $P=6.0$  kPa). The top boundary, shown in green in Fig. 2, also fixes the solid skeleton in the vertical direction. At the bottom boundary, shown in purple, the pore pressure is kept equal to zero. The pressure difference results in a hydraulic gradient of 0.6. Additionally, an erosion boundary condition, in terms of volumetric concentration ratio ( $n_e=0$ ), is applied to the top

boundary to prescribe clean water inflow (i.e., liquid carrying zero eroded mass). Lateral boundaries, shown in orange in Fig. 2, are impervious, fix the solid skeleton in the horizontal direction, and the gradient of volumetric concentration of fluidized grains is assumed to be zero.

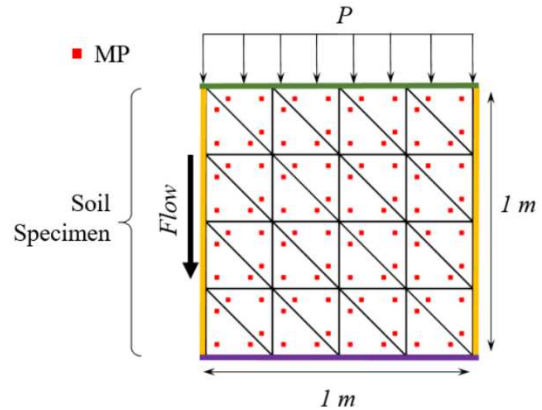


Figure 2. Sketch of the model and BCs for the SP approach.

##### 4.1 Double-point numerical model

This section covers the details specific to the DP model. The model is 2D with a soil block 1m tall by 1m wide. The nominal mesh size is 0.25m. The model is calculated with Material Point Integration (Al-Kafagi 2013). There is one SMP per element in the soil specimen, and their position is fixed at the corresponding Gauss Point.

Different models are run initially considering 3, 6, and 12 LMPs per element to study the effect of empty elements on the results (see Sec. 5). Empty elements are elements with SMPs but do not contain LMPs. This creates an artificial dry zone (within the saturated soil), and the erosion mechanism is not activated. The model with 12 LMPs per element is considered the base case.

Inflow and outflow boundaries based on Zhao et al (2019) are applied to inject free water into the system. New LMPs are generated in the inflow elements above the soil block. Simultaneously, when LMPs fall in the outflow elements below the soil specimen, these are removed from the system. The flow through the soil block is driven by applying a constant velocity of 0.12 m/s to the LMPs above the soil specimen. This velocity is consistent with the pressure boundary conditions applied in the SP approach, assuming laminar flow.

In the DP approach, the boundary between free liquid and saturated soil is the so-called transition zone (Martinelli 2016). The porosity in this boundary should be discontinuous ( $n_L=1$  in free fluid and  $n_L<1$  in saturated media). However, a continuous interpolated porosity field is required to evaluate porosity gradients from mass balances. In this example, to avoid any influence of the transition zones in the results, two lines of buffer elements are used immediately above and below the soil block. The buffer elements contain both LMP and SMP, but erosion is not allowed in these elements to ensure that the results of the model are consistent with the SP model.

Lateral boundaries, shown in orange in Fig. 3, are impervious and fixed in the horizontal direction. Erosion boundary conditions in terms of volumetric concentration ratio of fluidized grains are not required because the motion of liquid is tracked by LMPs. The concentration ratio of fluidized mass is automatically set to zero when LMPs are initialized in the inflow elements. The top and bottom of the model, shown in purple in Fig. 3, are fixed in the vertical and horizontal directions for both the liquid and solid phases.

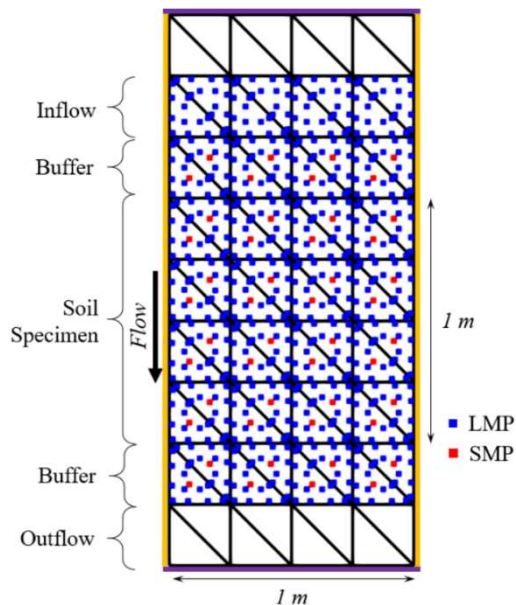


Figure 3. Sketch of the model and BCs for the DP approach. The model shown has 12 LMP per element as blue points and 1 SMP per element as red points. The computational background grid is shown in black.

## 5 NUMERICAL RESULTS AND DISCUSSION

This section presents the results obtained with the SP and DP models. Simplifications in terms of geometry and material properties allow the derivation of analytical solutions. The results for porosity ( $n_L$ ) vs. time for the SP, DP, and analytical solution are shown in Figure 4 below. The analytical solutions for the eroded mass are calculated by integrating the erosion laws (Eqs. 6 and 7) over the solid volume and over time. The results of both numerical approaches show excellent agreement with the analytical solution. Note that erosion is set to start after the first 2 seconds of calculation. A linear increase in porosity is observed for the constant erosion law (Eq. 6). After approximately 20 seconds, the erodible grains in the SMPs are completely eroded, and the maximum porosity ( $n_{L,max}=0.4$ ) is reached. Afterward, the porosity remains unchanged. The bottom set of lines present the results for the non-constant erosion law (Eq. 7). In this case, the porosity increases non-linearly and asymptotically tends to  $n_{L,max}$  as time evolves. The initial erosion rate is high but slows as the amount of remaining erodible mass in the SMPs decreases.

Figure 5 shows the results obtained with the DP approach considering 1, 3, and 12 LMPs per element. It is evident that the eroded mass vs. time for the DP formulation deviates with respect to the analytical solution when a small number of LMPs is considered. The reason for this discrepancy is presented in Figure 6, where the cumulative number of empty elements with time is presented. The simulation with the lowest number of LMPs accumulates the greatest number of empty elements. The simulation with 3 LMP per element shows significant improvement in the number of empty elements and the simulations with 12 LMP per element or greater do not have any empty elements during the runs. Based on these results, an optimum number of LMPs (in this model is 12 LMPs per element) is required to avoid the eventual occurrence of artificial dry elements and to ensure accurate results.

The SP approach does not suffer of “dry elements” because one of its fundamental assumptions is that MPs represent fully saturated porous media. In addition, for this particular analysis, the results are not sensitive to variations on the number of SMPs in the DP approach (or MPs in the SP approach) because the solid skeleton is assumed fixed. If the SMPs (or the MPs in the SP approach) were allowed to move, they would no longer be at the optimal Gauss point location in the element. This can decrease

the accuracy of the solution and one could expect some deviation between the numerical results and the analytical solution. Future investigation is needed to evaluate SP and DP approaches under these circumstances.

Finally, an essential aspect of numerical formulations is mass conservation, especially in those allowing for mass transfer among different constituents, such as the SP and DP approaches studied in this paper. Figure 7 shows the evolution of eroded mass, liquid mass, solid mass, and total mass obtained with the SP and DP formulations using constant and non-constant erosion laws. Results are compared with the analytical solution. All solutions present an excellent fit. The total mass in the system remains constant while the solid mass decreases, and the liquid and eroded masses increase with time.

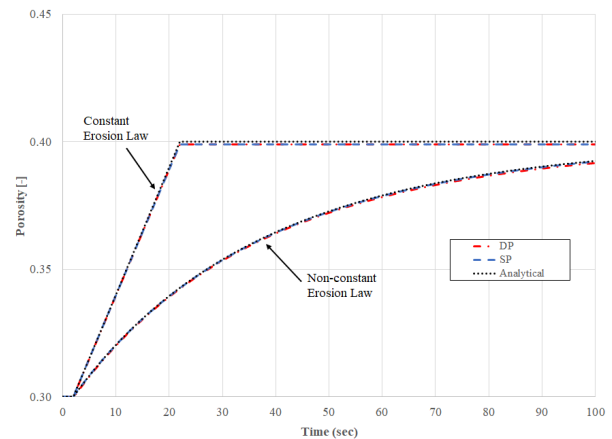


Figure 4. Porosity ( $n_L$ ) for SP and DP for both erosion laws vs time.

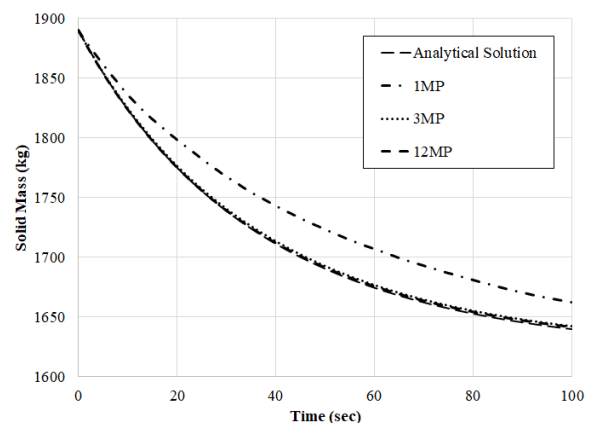


Figure 5. Total solid mass remaining in all SMPs for the DP model using three different numbers of LMPs vs time.

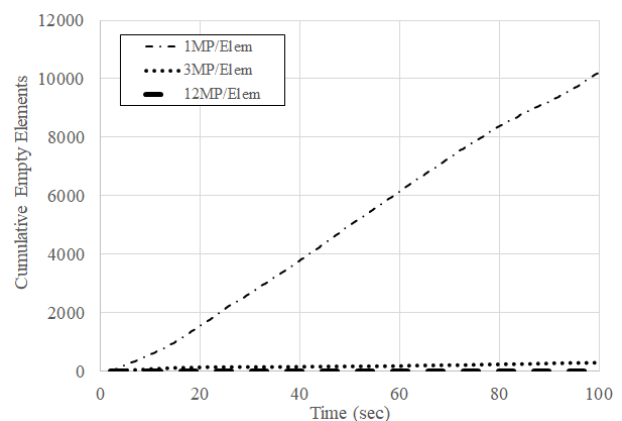


Figure 6. Cumulative empty elements vs. time for three different LMPs discretization.

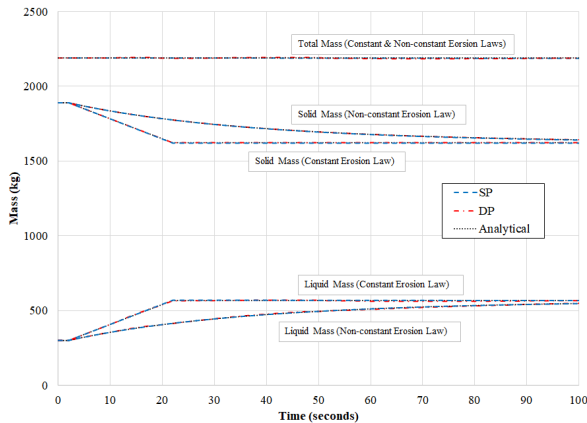


Figure 7. Mass balance for the SP and DP models for both erosion laws and the analytical solution.

## 6 CONCLUSIONS

The two MPM formulations proposed for the simulation of internal erosion of bimodal soils are presented. Both formulations are extensions of preexisting two-phase MPM frameworks, the so-called single-point (SP) and the double-point (DP). In particular, this paper shows the capabilities of both approaches for the study of internal erosion in bimodal when the internal structure of the soil remains intact (suffusion). One theoretical model of a constant-head suffusion test is used. Particular emphasis is placed on presenting the boundary conditions proposed in both models. Numerical results from both formulations fit well the analytical solution. The results are presented using two erosion laws. It is shown that the accuracy of the DP formulation is very sensitive to the discretization used for the liquid phase (number of LMPs). When different numbers of LMPs are initialized per element, the results show that there is a minimum number of LMPs required to ensure the accuracy of the solution. Otherwise, if the number of LMPs is too low, the occurrence of non-realistic dry elements in the saturated soil specimen leads to an underestimation of the eroded mass. The numerical results indicate that the mass conservation is fulfilled for both approaches. The SP approach does not suffer of this “dry elements” because the MPs are intrinsically fully saturated.

In general, the SP framework is more efficient because fewer MPs are required to perform the calculation. At the same time, the DP approach has the advantage that free water can be incorporated into the model, and a broader range of applications can be addressed. A limitation of the current approaches for the simulation of long-timescale processes is that the current implementations are explicit and are conditionally stable. Further validation is required to study the accuracy of the solution when large deformations of the solid skeleton are included in the model. The near future goal is to extend the erosion model to account for soil constitutive laws that account for the coupling between soil deformation and internal erosion.

## 7 REFERENCES

Al-Kafaji I.K.J. 2013. Formulation of a dynamic material point method (MPM) for geomechanical problems. *PhD Thesis*. Institut für Geotechnik der Universität Stuttgart, Germany.

Anura3D MPM Research Community. 2021. Anura3D MPM Research Community, [www.anura3D.com](http://www.anura3D.com).

Bandara, S. and Soga, K., 2015. Coupling of soil deformation and pore fluid flow using material point method. *Computers and geotechnics*, 63, 199-214.

Benseghier Z. Cuéllar P. Luu L-H. Bonelli S. and Philippe P. 2020. A parallel GPU-based computational framework for the

micromechanical analysis of geotechnical and erosion problems, *Computers and Geotechnics* 120, 103404.

Ceccato F. Yerro A. and Martinelli M. 2018. Modelling soil-water interaction with the material point method. Evaluation of single-point and double-point formulations. *Numerical Methods in Geotechnical Engineering IX*, CRC Press, Pp: 8.

Cividini A. and Gioda G. 2004 Finite-element approach to the erosion and transport of fine particles in granular soils. *International Journal of Geomechanics* 4(September): 191–198.

Fannin R.J. and Slangen P. 2014. On the distinct phenomena of suffusion and suffosion. *Géotechnique Letters* 4 (4), 289-294.

Indraratna B. Vo Trong N. and Rujikiatkamjorn C. 2011. Assessing the Potential of Internal Erosion and Suffusion of Granular Soils. *Journal of Geotechnical and Geoenvironmental Engineering* 137 (5), 550–554.

Lei S. He X. Chen H. Wong L. Wu E. and Liu A. 2020. Generalized interpolation material point method for modelling coupled seepage-erosion-deformation process within unsaturated soils. *Advances in Water Resources* 141: 666103578.

Martinelli M. 2016. Soil-water interaction with Material Point Method. Double-Point Formulation. *Report on EU-FP7 research project MPM-Dredge PIAP-GA-2012-324522*.

Murphy J. Yerro A. and Soga K. 2020. A New Approach to Simulate Suffusion Processes with MPM. *Geo-Congress 2020*. February 25–28, 2020, Minneapolis, Minnesota.

Richards K.S. and Reddy K.R. 2007. Critical appraisal of piping phenomena in earth dams. *Bulletin of Engineering Geology and the Environment* 66 (4), 381–402.

Skempton A.W. and Brogan J.M. 1994. Experiments on piping in sandy gravels. *Géotechnique* 44 (3), 449–460.

Soga K. Alonso E. Yerro A. Kumar K. and Bandara S. 2015. Trends in large-deformation analysis of landslide mass movements with particular emphasis on the material point method. *Géotechnique* 66(3): 248-273.

Stavropoulou M. Papanastasiou P. and Vardoulakis I. 1998. Coupled Wellbore Erosion and Stability Analysis. *International Journal for Numerical and Analytical Methods in Geomechanics* 769 (March 1997): 749–769.

Stepri D. 2003. Effects of the erosion and transport of fine particles due to seepage flow. *International Journal of Geomechanics* 3 (1), 111-122.

Subbiah S.K. Samsuri A. Mohamad-Hussein A. Jaafar M.Z. Chen Y.R. and Kumar R.R. 2020. Root cause of sand production and methodologies for prediction. *Petroleum*, ISSN 2405-6561 (In Press).

Sulsky D. Chen Z. and Schreyer H.L. 1994. A particle method for history-dependent materials. *Computer Methods in Applied Mechanics and Engineering* 118 (1-2): 179–196.

van Beek V.M. Bezuijen A. Sellmeijer J.B. and Barends F.B.J. 2014. Initiation of backward erosion piping in uniform sands. *Géotechnique* 64 (12): 927–941.

Vardoulakis I. Stavropoulou M. and Papanastasiou P. 1996. Hydro-mechanical aspects of the sand production problem. *Transport in Porous Media* 22, 225–244.

Wan R.G. and Wang J. 2002. Modelling Sand Production Within a Continuum Mechanics Framework. *Journal of Canadian Petroleum Technology* 41 (04), PETSOC-02-04-04.

Yerro A. Rohe A. and Soga K. 2017. Modelling Internal Erosion with the Material Point Method, *Procedia Engineering* 175: 365-372.

Zhao X. Bolognin M. Liang D. Rohe A. Vardon P. 2019. Development of in/outflow boundary conditions for MPM simulation of uniform and non-uniform open channel flows. *Computers & Fluids*, Volume 179, Pages 27-33.

Zhong C. Le V.T. Bendahmane F. and Marot D. 2018. Investigation of Spatial Scale Effects on Suffusion Susceptibility. *Journal of Geotechnical and Geoenvironmental Engineering* 144(9): 04018067.